



OPEN ACCESS

EDITED BY

Kiran F. Rajneesh,
The Ohio State University, United States

REVIEWED BY

Robert C. Wykes,
University College London, United Kingdom

*CORRESPONDENCE

Matthew A. Stern
✉ matthew.a.stern@emory.edu
Ken Berglund
✉ ken.berglund@emory.edu

RECEIVED 16 July 2024

ACCEPTED 13 August 2024

PUBLISHED 29 August 2024

CITATION

Stern MA, Dingledine R, Gross RE and Berglund K (2024) Epilepsy insights revealed by intravital functional optical imaging. *Front. Neurol.* 15:1465232. doi: 10.3389/fneur.2024.1465232

COPYRIGHT

© 2024 Stern, Dingledine, Gross and Berglund. This is an open-access article distributed under the terms of the [Creative Commons Attribution License \(CC BY\)](https://creativecommons.org/licenses/by/4.0/). The use, distribution or reproduction in other forums is permitted, provided the original author(s) and the copyright owner(s) are credited and that the original publication in this journal is cited, in accordance with accepted academic practice. No use, distribution or reproduction is permitted which does not comply with these terms.

Epilepsy insights revealed by intravital functional optical imaging

Matthew A. Stern^{1*}, Raymond Dingledine², Robert E. Gross^{1,3} and Ken Berglund^{1*}

¹Department of Neurosurgery, Emory University School of Medicine, Atlanta, GA, United States, ²Department of Pharmacology and Chemical Biology, Emory University School of Medicine, Atlanta, GA, United States, ³Department of Neurological Surgery, Rutgers Robert Wood Johnson Medical School, New Brunswick, NJ, United States

Despite an abundance of pharmacologic and surgical epilepsy treatments, there remain millions of patients suffering from poorly controlled seizures. One approach to closing this treatment gap may be found through a deeper mechanistic understanding of the network alterations that underly this aberrant activity. Functional optical imaging in vertebrate models provides powerful advantages to this end, enabling the spatiotemporal acquisition of individual neuron activity patterns across multiple seizures. This coupled with the advent of genetically encoded indicators, be them for specific ions, neurotransmitters or voltage, grants researchers unparalleled access to the intact nervous system. Here, we will review how *in vivo* functional optical imaging in various vertebrate seizure models has advanced our knowledge of seizure dynamics, principally seizure initiation, propagation and termination.

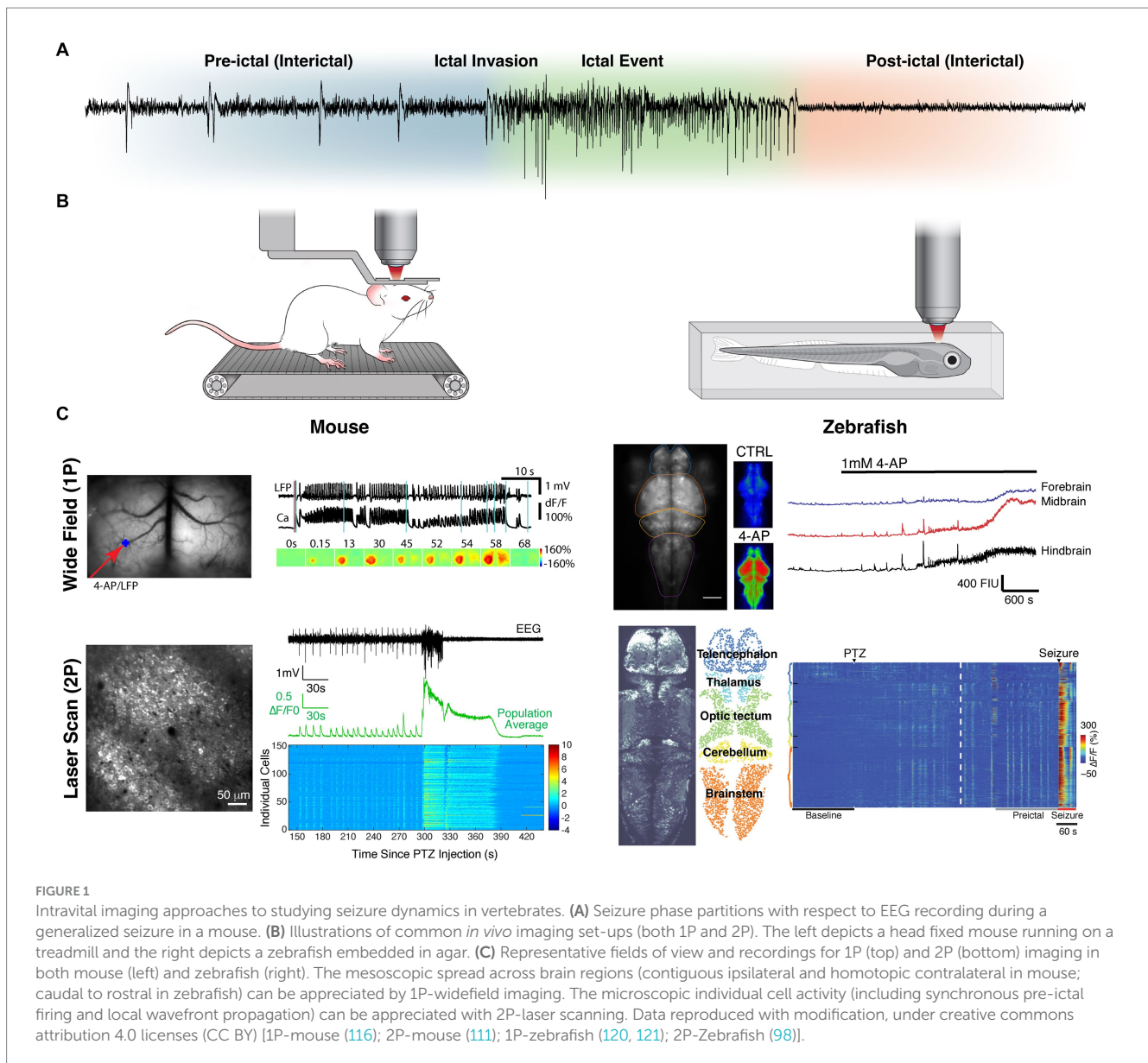
KEYWORDS

seizure, two-photon, widefield, light sheet, GECI, GEVI, *in vivo* imaging, neurophotonic

Introduction

Epilepsy, a serious health condition characterized by recurrent and often disabling seizures (1–3), is the fourth most common neurological disorder (4), with prevalence ranging from 0.5 to 1% around the world (5, 6). Despite over a century of drug development (7), about one third of these cases are medically intractable (8–10). This is perhaps in part due to the approach often taken, agnostic to seizure microcircuitry and network physiology. Surgical interventions such as ablation (11, 12), open resection (13, 14), and electrical stimulation (15, 16) are sometimes options for pharmacoresistant epilepsy. However, none of these procedures render all patients seizure free. Additionally, they can result in off-target effects, and are generally unavailable in developing countries. Thus, a significant need exists for more targeted and effective therapies (17, 18). A deeper understanding of the role of individual neurons, neuronal ensembles, and neural networks in initiating, propagating and terminating epileptic discharges underlying seizures would facilitate such advances.

Currently, the bulk of our knowledge of seizure dynamics comes from macroelectrode population electrophysiology, with electroencephalography (EEG; Figure 1A) having demonstrated that seizure activity can spread from a focal brain region in a diffuse yet stereotyped network (19). However, this approach fails to capture the complex underlying microcircuit dynamics, many permutations of which can result in the same recorded signal (18). To characterize seizure dissemination between individual neurons, single unit recordings



have been performed in humans and animals using microelectrode arrays (MEAs). These recordings have shown that firing and termination of firing of neurons recruited during seizures is highly synchronous and stereotyped (20, 21), where ictal wavefronts propagate with similar directionality across seizures and interictal spikes propagate in antiparallel fashion (22). Additionally, electrophysiology combined with GABAergic pharmacology has been used to find evidence of inhibitory networks restraining seizure activity, including surround and feedforward inhibition (23, 24). However, these recordings have limited recording density, typically at a single cortical depth, due to their planar configuration of sparsely arranged contacts. Furthermore, it is generally impossible to know the subtype of neuron being recorded [for exceptions see (25, 26)]. Moreover, it is challenging to determine if the activity being recorded emanates from the same neuron between separate recording sessions.

Functional optical imaging in animal models (Figure 1B) circumvents many of the limitations of electrophysiology and allows for observation of activity of substantially more neurons. Calcium

(27–30) or voltage sensitive dyes (31, 32) were originally used for this purpose, but were rarely cell-type selective, and disadvantaged by significant photobleaching, poor intracellular retention and toxicity (33). The development of genetically encoded indicators, expressed either through viral transduction or through genetic model development, has enabled cell-type specific imaging. These fluorescent proteins undergo a conformational change to excitable states upon the binding of specific ions or small molecules (34, 35). The most commonly used indicators are genetically encoded calcium indicators (GECIs) that fluoresce in the presence of calcium (35–41). They can serve as proxies for neuronal firing, which is marked by an increase of intracellular calcium. In addition to calcium, a growing arsenal of genetically encoded indicators are being developed (34, 42), including for other ions (43–48), small molecules and neurotransmitters (49–58). Furthermore, genetically encoded voltage indicators (GEVIs) have been developed, exploiting voltage-sensitive domains (59–63).

For imaging, these indicators can be excited with either a single photon (1P) in the visible range or two (or more) coincident photons

in the infrared range. While 1P excitation can be achieved with many intravital microscope setups, including epifluorescence widefield, laser scanning confocal and light sheet, 2P necessitates the use of a femtosecond mode-locked laser for light delivery (64). Consequently, 2P imaging is limited to laser scanning, although a few light sheet uses exist (65). The temporal and spatial resolution of these methods varies greatly (17, 64, 66–68) and thus the selection of the method should be tailored to the question and indicator. 1P widefield imaging offers the largest fields of view with fastest temporal resolution (Figure 1C). However, for investigations looking at subcellular compartments or multiple cell populations of tens to hundreds of individual neurons, 2P laser scanning is often best. For questions related to brain-wide mesoscale networks, light sheet and 2P laser scanning in transparent zebrafish larva have been the methods most often used. All the above methods require head fixing or immobilizing the subject under an objective. Should the question necessitate a wider range of behavior or longer imaging session, head mounted microscopes [1P (69) and 2P (70, 71)] can be used in freely moving mice. For a more detailed review of epilepsy intravital imaging methodology see (66).

Since the first intravital optical imaging study using a genetically encoded indicator in a vertebrate seizure model nearly a decade ago (72) there have been over 50 additional such studies published. These have sought to examine the contributions of different cell types and neurotransmission to seizure dynamics, the reliability of initiation and propagation patterns, the network changes in synchrony and connectivity that occur at micro and macroscale, and the impact of this aberrant activity on normal function. This review will serve to summarize the major contributions these investigations have provided to our understanding of seizure physiology.

Overview

Seizures can be partitioned into several distinct phases, namely interictal, pre-ictal, ictal, and post-ictal (Figure 1A). While each phase's distinct dynamics are of importance, it is the evolution of that activity and the transitions between phases that are often the focus of investigation. Therefore, we have organized our review in a complementary fashion. Table 1 lists the *in vivo* imaging studies included in this review, specifically those that used genetically encoded indicators to investigate epileptiform activity directly. Experiments where imaging was not *in vivo* (e.g., *ex vivo* slice), used dyes, or was only performed during non-epileptiform activity are not discussed.

Interictal activity

Interictal spikes (IIS) are episodes of transient synchronous paroxysmal depolarization across ensembles of hyperexcitable neurons, classically observed as a spike wave discharge on EEG (73). Widefield imaging of the cortex has demonstrated that IIS begin as standing waves in local regions with limited contiguous spread (74), although some cortex-wide propagation and delayed recruitment of distal non-contiguous foci has been observed (75, 76). While IIS are often limited to or emanating from the purported epileptic focus, in instances of extrafocal origin, or non-contiguous spread, these loci often share homotopic connection with the ictal

focus (74, 77). These patterns have been observed in both excitatory and inhibitory populations (77). The local and limited nature of interictal activity is corroborated by whole brain imaging in zebrafish (78–80).

To parse the individual cell activity patterns underlying IIS, laser scanning microscopy was employed. Imaging the zebrafish optic tectum revealed hypersynchronous recruitment of microensembles underlying the spatially confined interictal activity observed by previous studies with widefield microscopy (79, 81). In the pilocarpine chronic seizure mouse model, it was shown that inhibitory neurons are disproportionately active relative to pyramidal cells during IIS in CA1, consistent with a perisomatic inhibitory restraint occurring. Additionally, while it seems there are subpopulations of neurons consistently active together, their recruitment is varied across spikes (72). However, in a chronic intrahippocampal kainic acid (KA) mouse model, synchronous bursts of pyramidal cells have been observed, which could speak to model differences in ictogenic mechanisms (82). When imaging the dentate gyrus (DG) also following intrahippocampal KA, distinct microensembles of excitatory adult born granule cells (abGCs) were determined to overly drive IIS, albeit firing in a desynchronized manner. The specific ensembles recruited across IIS were varied. These are distinct from the microensembles that participate in sharp wave ripples, which were shown to be driven by both mature and abGCs, firing with greater synchrony. This suggests that decoupling of abGCs from mature GCs and subsequent reorganization into these desynchronized pathologic ensembles may contribute to an impairment in dentate gating, enabling ictogenesis (83). When training computational models on calcium data from this model, abGCs were most often identified as superhub neurons with high feedforward conductance, enhancing downstream excitation in the resulting epileptic networks (84). Neurons outside the hippocampus, but still part of this network have also been found to be involved in seizure regulation, such as the fasciola cinereum, a collateral intermediary nucleus connecting the entorhinal cortex to the DG (85). Gap junctions may be in part mediating the spread of IIS activity, particularly in the astrocyte syncytium, as blocking gap junctions significantly decreased the occurrence, duration and spread of IIS (79). However, while astrocytes in CA1 exhibit transient increases in calcium spontaneously during the interictal period, these have been observed asynchronous with IIS (86).

For those spikes occurring in the cortex there is a notable recruitment of pyramidal cells (87, 88), limited to layer II/III, in addition to inhibitory cells (89). While both parvalbumin (PV) and somatostatin (SST) cells demonstrate activity during IIS, PV cells were predominantly recruited with a higher degree of inter- (with pyramidal cells) and intrapopulation synchrony, while SST cells demonstrated asynchronous and delayed recruitment (89). Combined GEVI and GECI imaging in pyramidal cells revealed that there is little supra- or subthreshold activity propagating out of the focus during IIS (90). Studies utilizing neurotransmitter indicators were concordant with these IIS dynamics, revealing an increase in glutamate observed at the focus, which expanded centrifugally, and an increase in gamma-aminobutyric acid (GABA) observed extrafocally, which displayed slower and more persistent centripetal propagation, consistent with intact feedforward inhibitory surround limiting the IIS spread (51, 91). Indeed, the IIS may reflect this restraining mechanism (92). Importantly, the majority of these studies were performed in focal neocortical models, where a chemoconvulsant was intracortically

TABLE 1 Intravital functional optical imaging seizure studies using genetically expressed indicators.

First author	Year	Journal	Method	Species	Model	FOV	Cell type	Indicator type	Seizure phase			
									IIS	Pre-ictal	Ictal	Post-ictal
Deng (54)	2024	Nat Methods	1P-Widefield	Mouse	KA (i.p.)	Ctx	Extracellular	Ca, 5-HT, eCB				•
Jamiolkowski (85)	2024	Nat Med	2P-Laser Scan	Mouse	KA (d. hipp)	FC (Hipp)	FC cells	Ca	•			
Lau (125)	2024	Epilepsia	1P-Miniscopes	Mouse	APP/PS1 Cortical Injury	CA1 (Hipp)	Pan-neuronal	Ca		•	•	
Li (93)	2024	J Cereb Blood Flow Met	1P-Widefield	Mouse	BIC	Ctx	Pyramidal	Ca	•			
Nguyen (127)	2024	Nat Commun	2P-Laser Scan	Mouse	Electrical kindling (hipp), KA (d. hipp)	CA1 (Hipp)	Pan-neuronal, extracellular	Ca, ACh			•	
Shah (114)	2024	Cell Rep	1P-Widefield, 2P-Laser Scan	Mouse	4-AP	Ctx (II/III)	Pan-neuronal + Nkx2.1 (PV, SST) reporter	Ca	•		•	
Stern (111)	2024	Neurophotonics	2P-Laser Scan	Mouse	PTZ	Ctx (II/III)	VGAT + non-VGAT	Ca		•	•	•
Burrows (105)	2023	J Neurosci	2P-Laser Scan	Zebrafish	PTZ	WB	Pan-neuronal	Ca		•	•	
Li (88)	2023	iScience	2P-Laser Scan	Mouse	scn2a + PTZ	Ctx (V)	Pyramidal	Ca	•			
Luo (77)	2023	Epilepsia	1P-Widefield	Mouse	BIC	Ctx	Pyramidal, PV	Ca	•			
Masala (82)	2023	Brain	2P-Laser Scan	Mouse	KA (d. hipp)	CA1 (Hipp)	Pyramidal	Ca	•			
Shimoda (91)	2023	Brain	2p-Spiral Linescan	Mouse	4-AP, Ptx	Ctx (I)	Extracellular	GABA, Glu	•	•		
de Vito (118)	2022	Biomed Opt Express	2P-Light Sheet, 1P-Widefield	Zebrafish	PTZ	WB	Pan-neuronal	Ca			•	•
Dong (56)	2022	Nat Biotechnol	2P-Laser Scan	Mouse	Electrical kindling (v. hipp)	CA1 (Hipp)	Pan-neuronal, extracellular	Ca, eCB			•	•
Hotz (100)	2022	Glia	1P-Widefield, 2P-Laser Scan	Zebrafish	PTZ, <i>eaat2a</i> + photostim	WB	Pan-neuronal, astroglial	Ca, Glu		•	•	
Mulcahey (108)	2022	eNeuro	2P-Laser Scan + Transparent MEA	Mouse	4-AP	CA1 (Hipp)	Pyramidal	Ca			•	
Myren-Svelstad (101)	2022	Epilepsia	2P-Laser Scan	Zebrafish	PTZ, <i>eaat2a</i> , <i>gabral1</i> + photostim	WB	Pan-neuronal, astroglial	Ca		•	•	•
Niemeyer (80)	2022	Brain	2P-Laser Scan	Zebrafish	PTZ	WB	Pan-neuronal + VGLUT2 reporter	Ca	•	•	•	
Özsoy (119)	2022	Front Mol Neurosci	1P-Widefield, Photoacoustic	Zebrafish	<i>eaat2a</i> + photostim	WB	Pan-neuronal	Ca			•	
Turrini (99)	2022	Biomedicines	2P-Light Sheet	Zebrafish	PTZ	WB	Pan-neuronal	Ca		•	•	•
Zhang (109)	2022	Neurosci Bull	2P-Miniscopes	Mouse	KA (i.p.)	Ctx*	Pan-neuronal	Ca		•	•	•

(Continued)

TABLE 1 (Continued)

First author	Year	Journal	Method	Species	Model	FOV	Cell type	Indicator type	Seizure phase			
									IIS	Pre-ictal	Ictal	Post-ictal
Bando (90)	2021	Nat Commun	2P-Laser Scan	Mouse	4-AP	Ctx (I-VI)	Pyramidal	Ca, Voltage	•	•	•	
Driscoll (107)	2021	Commun Biol	1P-Widefield + Transparent MEA	Mouse	4-AP	Ctx	Pyramidal	Ca			•	
Farrell (126)	2021	Neuron	2P-Laser Scan	Mouse	Electrical kindling (v. hipp)	CA1 (Hipp)	Pan-neuronal, extracellular	Ca, eCB			•	
Hadjibadi (84)	2021	Neuron	2P-Laser Scan	Zebrafish; Mouse	PTZ; KA (v. hipp)	WB; DG (Hipp)	Pan-neuronal; GCs + abGC reporter	Ca	•	•	•	
Lim (103)	2021	J Cereb Blood Flow Met	2P-Laser Scan	Mouse	4-AP	Ctx (II/III)	Pyramidal, GABAergic	Ca		•	•	
Liu (79)	2021	iScience	1P-Spinning disc	Zebrafish	<i>stxbp1p</i>	WB	Pan-neuronal	Ca	•			
Somarowthu (115)	2021	Cell Calcium	2P-Laser Scan	Mouse	<i>scn1a</i> + Heat	Ctx*	Pan-neuronal + PV, SST, VIP reporters	Ca		•	•	
Wong (110)	2021	Neuropsychopharmacology	1P-Miniscopes	Mouse	<i>scn8a</i> + PTZ	Ctx	Pyramidal	Ca			•	
Yang (116)	2021	Front Neurosci	1P-Widefield	Mouse	4-AP	Ctx	Pyramidal	Ca			•	•
Aeed (89)	2020	Ann Neurol	2P-Laser Scan	Mouse	4-AP	Ctx (II/III, V)	Pyramidal; PV; SST (separate)	Ca	•	•	•	
Cozzolino (78)	2020	Cells	2P-Laser Scan	Zebrafish	PTZ; <i>kcj10a</i>	WB	Pan-neuronal	Ca	•	•		
Farrell (124)	2020	Sci Rep	2P-Laser Scan	Mouse	Electrical kindling (v. hipp)	CA1 (Hipp)	Pyramidal	Ca			•	•
Hatcher (117)	2020	J Clin Invest	1P-Widefield	Mouse	Glioma	Ctx	Pan-neuronal	Ca			•	•
Montgomery (76)	2020	Cell Rep	1P-Widefield, 2P-Laser Scan	Mouse	Glioma	Ctx	Pyramidal	Ca	•		•	
Shuman (94)	2020	Nat Neurosci	1P-Miniscopes	Mouse	Pilo (I.P.)	CA1 (Hipp)	Pan-neuronal	Ca	•			
Sparks (83)	2020	Nat Commun	2P-Laser Scan	Mouse	KA (v. hipp)	DG (Hipp)	Pan-neuronal + abGC reporter	Ca	•			
Tran (131)	2020	JCI Insight	2P-Laser Scan	Mouse	Max electroshock	Ctx*	Astroglial, mural	Ca				•
Tran (102)	2020	J Neurosci	2P-Laser Scan	Mouse	<i>scn1a</i> + Heat	Ctx (II/III)	Pan-neuronal + PV reporter	Ca		•	•	•
Brenet (96)	2019	Cells	1P-Widefield	Zebrafish	<i>scn1a</i>	WB	Pan-neuronal	Ca			•	
Jayant (112)	2019	Cell Rep	2P-Laser Scan + Nanopipette	Mouse	4-AP	Ctx (II/III)	Pyramidal	Ca		•	•	

(Continued)

TABLE 1 (Continued)

First author	Year	Journal	Method	Species	Model	FOV	Cell type	Indicator type	Seizure phase			
									IIS	Pre-ictal	Ictal	Post-ictal
Liao (97)	2019	Dis Model Mech	1P-Spinning Disc; 1P-Light Sheet	Zebrafish	<i>gabrg2</i> + photostim	WB	Pan-neuronal	Ca			•	
Liu (81)	2019	eNeuro	2P-Laser Scan	Zebrafish	PTZ, 4-AP	WB	Pan-neuronal	Ca	•	•	•	
Marvin (51)	2019	Nat Methods	2P-Laser Scan	Mouse	Pilo (ctx)	Ctx (II/III)	Extracellular	GABA	•			
Verdugo (98)	2019	Nat Commun	2P-Laser Scan	Zebrafish	PTZ	WB	Pan-neuronal, astroglial, extracellular	Ca, Glu		•	•	
Wenzel (95)	2019	J Neurosci	2P-Laser Scan	Mouse	4-AP	Ctx (II/III)	Pan-neuronal + PV reporter	Ca		•	•	
Heuser (86)	2018	Cereb Cortex	2P-Laser Scan	Mouse	KA (i.p.)	CA1 (Hipp)	Pan-neuronal, astroglial	Ca	•		•	•
Liou (23)	2018	Brain	2P-Laser Scan	Mouse	4-AP	Ctx (II/III)	PV	Ca		•		
Meyer (122)	2018	Nat Commun	2P-Laser Scan	Mouse	<i>stargazer</i>	Ctx (II/III-VI)	Pan-neuronal + IHC reporters	Ca		•	•	
Rosch (104)	2018	PLoS Comput Biol	1P-Light Sheet	Zebrafish	PTZ	WB	Pan-neuronal	Ca		•		
Zhang (106)	2018	Nano Lett	2P-Laser Scan + transparent MEA	Mouse	4-AP	Ctx*	Pyramidal	Ca			•	
Petrucchio (87)	2017	Sci Rep	2P-Laser Scan	Mouse	BIC	Ctx (II/III)	Pyramidal	Ca	•			
Rossi (74)	2017	Nat Commun	1P-Widefield	Mouse	Pilo, Ptx	Ctx	Pan-neuronal, pyramidal	Ca	•		•	
Sato (44)	2017	Proc Natl Acad Sci	2P-Laser Scan	Mouse	4-AP	Ctx (II/III)	CAG-promoter	Cl, pH			•	•
Steinmetz (75)	2017	eNeuro	1P-Widefield	Mouse	various transgenics	Ctx	various	Ca	•			
Turrini (120)	2017	Sci Rep	1P-Widefield	Zebrafish	PTZ	WB	Pan-neuronal	Ca		•	•	
Wenzel (113)	2017	Cell Rep	2P-Laser Scan	Mouse	4-AP, Pilo	Ctx (II/III, V)	Pan-neuronal	Ca			•	
Winter (121)	2017	Sci Rep	1P-Light Sheet, 1P-Widefield	Zebrafish	PTZ, 4-AP, Pilo, Strychnine	WB	Pan-neuronal	Ca			•	
Berdyeva (123)	2016	Front Neurosci	1P-Miniscope	Mouse	KA (i.p.); NMDA; PTZ	CA1 (Hipp)	Pyramidal	Ca			•	•
Muldoon (72)	2015	Brain	2P-Laser Scan	Mouse	Pilo	CA1 (Hipp)	Pan-neuronal, GABAergic	Ca	•			

1P, one-photon; 2P, two-photon; 4-AP, 4-aminopyridine; 5-HT, 5-hydroxytryptamine (serotonin); BIC, bicuculline; Ca, calcium; Ctx, cortex; DG, dentate gyrus; eCB, endocannabinoid; FC, fasciola cinereum; GABA, gamma-aminobutyric acid; GC, granule cell (ab, adult born; m, mature); Glu, glutamate; Hipp, hippocampus (d, dorsal; v, ventral); IHC, immunohistochemistry; i.p., intraperitoneal; KA, kainic acid; NMDA, N-methyl-D-aspartate; Pilo, pilocarpine; Ptx, picrotoxin, PTZ, pentylenetetrazol; PV, parvalbumin; SST, somatostatin; VGAT, vesicular GABA transporter; VGLUT, vesicular glutamate transporter; VIP, vasoactive intestinal peptide; WB, whole brain; *Imaging depth/layer not reported; Italics indicate transgenic line.

injected to elicit epileptiform activity. Corroborating studies across other models could strengthen the generalizability of these findings.

Combined widefield GECI imaging with optical imaging of intrinsic hemodynamic signal to examine neurovascular coupling showed that during IIS there is an initial 'epileptic' dip in hemoglobin oxygenation, likely the result of vasodilation, followed by a period of hyperoxygenation, due to increased levels of total hemoglobin delivery, all of which is tightly spatially correlated with excitatory cell activation (76, 93).

In terms of functional impact, hippocampal place cell encoding is impaired in two chronic seizure models, with aberrant dendritic hyperexcitability (82) and aberrant firing and desynchronization (94) hypothesized as contributing mechanisms.

Taken together, intravital imaging at microcircuit resolution has revealed distinct cell type activity patterns specific to different anatomical regions during IIS, and speaks also to intra- vs. extrafocal differences (92). There is considerable variability in the specific neurons recruited, where different ensembles can be recruited across sequential IISs.

Pre-ictal to ictal transition

Interictal periods, by definition, occur between seizures and thus they have both pre-ictal and post-ictal phases, the exact boundaries of which are poorly defined. Thus, to examine the pre-ictal phase, we look at the interictal period from the perspective of the progression of dynamic changes as the brain state transitions to seizure.

An advantage of imaging is the ability to delineate activity as intra- or extrafocal. When recording from the focus in a mouse 4-aminopyridine (4-AP) model, recruitment of both excitatory and inhibitory neurons in local microensembles, akin to microseizures, was observed prior to ictal onset. As the brain progressed to seizure, ensemble activity increased across populations, with synchronization amongst excitatory cells (95). When examining dynamics at mesoscales in zebrafish whole brain, the mesencephalon/optic tectum, and occasionally the thalamus, emerged as a conserved region of hyperactivity (96–98) and seizure focus (78, 80, 81, 99–101). It was found that foci tended to have a higher proportion of excitatory cells than in the penumbra, perhaps contributing to their hyperexcitability (80).

When exploring cortical regions outside of the seizure onset zone prior to seizure invasion, feedforward inhibitory activity was observed, be it increased firing activity of inhibitory neurons (23, 95, 102, 103), or elevated GABA release during pre-ictal spikes relative to within the focus (91). Excitatory recruitment was still discernable, although possibly with some degree of suppression (95). As the tissue transitioned to a seizure state, there was a progressive increase in synchronization amongst pyramidal cells (89, 102), with a gradual breakdown in the inhibitory surround, witnessed as desynchronization in the PV cells activity (89, 102) and a decrease in released GABA during spiking (91). Inhibitory restraint weakening is also detected as progressively increasing bursts of subthreshold activity in pyramidal cells by GEVI imaging in the penumbra (90). As compared with neurons, astroglial networks displayed a more widespread elevation in calcium activity and synchrony pre-ictally, although their bursts of activity seemed to follow immediately after neuronal bursts during pre-ictal spikes (98).

Modeling based upon whole brain zebrafish mesoscale 1P light sheet imaging during PTZ induced seizures found that the tectum served as a networkwide hub. As the brain transitioned to seizure, there was a decrease in input to the tectum, enabling downstream network synchronization. The brain-wide recruitment was facilitated by increasing faster excitatory transmission and decreasing slower inhibitory transmission (104). Similar findings emerged from a model trained on 2P data with single-cell resolution collected from the same model. Specifically, they found that pre-ictal networks had enriched feedforward motif conductance, especially amongst "superhub" neurons, which promoted the pro-seizure tendency of the network (84). Another computational study using 2P data in the same model estimated microscale avalanche dynamics and showed that there was an increase in network connectivity at single-cell resolution, which drove the brain away from criticality, a point of maximal flexibility in brain state, thus limiting phase transition possibilities until the system converged on an inflexible ictal state (105).

Seizure propagation and ictal dynamics

Upon seizure invasion, suprathreshold activity is observed, first as a fast voltage wave and then a slower calcium wave (0.5–1 s delay) (90). Simultaneous calcium imaging through transparent microelectrode and electrocorticography arrays demonstrate spatial concordance between the modalities (106), where progression of ictal electrophysiology is tied with expansion of ictal core (107, 108).

Highly elevated and sustained calcium can be detected (109, 110) in both excitatory cells and inhibitory neurons (95, 102, 111), with pyramidal cells displaying the greatest recruitment and hypersynchrony (80, 89, 103). A concordant expansion of glutamate release into the field is also observed (91, 100), hypothesized to be in part released by glia (98). However, while calcium amplitude is classically thought to be directly correlated with activity, a large increase could also indicate intracellular calcium homeostasis breakdown, and thus an absence of firing. A simultaneous *in vivo* imaging and patch clamp study revealed that the PV cells with an ictal calcium increase, actually enter a state of depolarization block upon seizure invasion (112), consistent with inhibitory restraint collapse.

Propagation can be witnessed as a calcium wavefront (102, 111, 113), yet the recruitment of interneurons within this seems variable. In the 4-AP model the PV neuron recruitment appears spatially heterogeneous (95) at invasion, with a delayed recruitment in SST cells (89). However, in a study imaging Nkx2.1 cells (PV and SST), these were found to be recruited in a spatiotemporally concordant manner to the other cells in the field (114). In a Dravet mouse model with thermally induced seizures, PV and vasoactive intestinal peptide-expressing (VIP) cells appear recruited along with the population, while SST cells demonstrate a spatially independent early recruitment (115). With respect to cortical layers, layer II/III pyramidal cells tend to be the first to propagate during the seizure, with a lagging recruitment of layer V (89, 113). The propagation has also been found to have reliable recruitment across sequential ictal events following intracortical injection of a chemoconvulsant (95, 113). The speed of propagation varied across events, although when the cortex had been first disinhibited by picrotoxin, the speed increased and variability was dampened, consistent with the inhibitory restraint hypothesis (113).

Interestingly, in a study where optogenetic photostimulation during calcium imaging was used to determine excitability in individual cells, decreased excitability proximal to the invading seizure wavefront was observed, in contrast to hyperexcitability observed interictally and baseline level excitability observed distal to invasion, suggesting that inhibitory neurons recruited to the seizure generate a front of local inhibition (114).

Propagation through brain regions appears to follow both proximal contiguous and distal homotopic spread with respect to the onset zone (74), including contralateral projections (76, 116, 117). In zebrafish, whole brain propagation was found to typically occur caudal to rostral (78, 100, 118, 119), although the opposite direction was occasionally observed (81), perhaps related to the different developmental stage and chemoconvulsant dosage used (118). While activity in rostral regions (telencephalon and habenula) is not initially correlated with the caudal regions (optic tectum, cerebellum and medulla), entrainment occurs along the rostrocaudal axis upon progression to seizure (98, 99, 120). Indeed, eventually the brain-wide synchrony can be observed (81, 84, 97, 104, 118), although there is some model dependency on the exact extent of recruitment (101, 121). The astroglial syncytium's calcium activity also displays brain-wide hyperactivity (100) and synchrony within itself and with neurons during seizures (98). There is, though, a short delay in the astroglial ictal recruitment (101), corresponding to a further increase in neural activity, consistent with the hypothesis that neural activity is exacerbated by glial glutamate release (98). Impaired glutamate reuptake by astrocytes also led to hyperexcitability with spontaneous seizures and concurrent excessive glutamate signal (100). At seizure invasion, there is a large increase in intracellular chloride that slowly builds throughout the seizure, while pH slightly decreases (44).

Interestingly, imaging in the visual cortex of a mouse absence model revealed an opposite finding to the other seizure models, a decrease in neuronal activity and synchronization across cortical layers and neuron subtypes during ictal episodes. This asynchronous suppression could be related to the impaired visual awareness classically associated with this seizure type (122).

In the hippocampus, ictal activity shows recruitment in both CA1 pyramidal cells (123, 124), as well as the fasciola cinereum (85). While recruitment is highly synchronous for many neurons at invasion, new neurons are continuously recruited throughout the seizure (125). Spatial propagation dynamics recapitulated those of the cortex, demonstrating within-subject reliability for sequential events and a much faster expansion of electrophysiologic signatures ahead of the neuronal recruitment to the propagating calcium wave (108). Additionally, spatiotemporally concordant release of endocannabinoids occurs, which may play a feedback role in restricting seizure activity (56, 126). Acetylcholine levels have also been shown to increase during seizures, strongly correlating with intracellular calcium (127). Astrocytic calcium increased during seizure invasion as well, sometimes preceding the event, which may be in part mediated by internal store release (86).

With respect to neurovascular coupling, while the ictal focus is typically well supplied and only occasionally hypoxic, the penumbra is hyperoxygenated during seizure initiation and propagation, extending beyond the recruited tissue. At initiation, the blood supply to the focus increases, and this expansion appears as a wave ahead of the calcium wave in neurons into the penumbra and persists into the post-ictal phase (76, 116).

Seizure termination and post-ictal activity

Upon seizure termination or shortly into the post-ictal period, slow propagating waves of calcium have been recorded in the cortex (54, 102, 109, 111, 117) and hippocampus (56, 86, 123, 124). These waves have been hypothesized to be spreading depolarizations as they share similar spatiotemporal propagation properties (128), and spreading depolarizations can be temporally associated with seizures (129, 130). Spatiotemporally concordant serotonin and endocannabinoids waves have also been detected during these calcium waves (54, 56). These calcium waves are then followed by periods of post-ictal suppression of activity and synchrony (118, 124), with one zebrafish study showing functional connectivity to bifurcate into rostral and caudal groups (99). Intracellular chloride returns to baseline levels upon seizure termination and a gradual intracellular acidification occurs post-ictally (44).

A transient increase in astrocytic calcium was also observed post-ictally (86), corresponding to post-ictal vasoconstriction (131), as well as post-ictal hypoactivity (101). While this glial calcium level was sustained for at most a few minutes, vasoconstriction was observed for over an hour. Vasculature smooth muscle cells also showed elevated calcium for the duration of the vasoconstriction (131). When post-ictal vasoconstriction was depressed by a COX-2 inhibitor, the duration of astrocytic calcium elevation was significantly diminished (131), while post-ictal suppression or recovery of neural activity was unchanged (124). On the other hand, when glia glutamate reuptake was impaired, post-ictal hypoactivity was diminished (101). Taken together, a vascular coupling to neuronal and glial activity is present post-ictally, although there may be a dissociation from their post-ictal suppressive mechanisms.

Looking forward

Intravital microscopy coupled with genetically targeted indicators has allowed unprecedented access to the intact nervous system. Leveraging these powerful tools across a variety of vertebrate seizure models has provided deep insight into mechanisms of epilepsy. Imaging has confirmed previous hypotheses derived from electrophysiology, such as the existence of microseizures inside an epileptic focus (132, 133) and the role of inhibition in restraining seizure activity (19, 24, 134). Imaging has also enabled new discoveries which have opened possibilities for novel treatment targets and approaches to epilepsy (17, 135), such as the neuromodulation of adult-born dentate granule cell superhubs (84), or leveraging seizure specific neurochemical changes for drug design (127), which could be extended as an autoregulatory gene therapy (136). Optical and genetic technologies are advancing quickly, opening even more possibilities. Already there are methods that could allow imaging of the whole cortex at a single cell resolution (137, 138), that enable imaging deeper in the brain without the need to aspirate the cortex (139), that capture activity in freely moving subjects to better tie behavior to ensemble activity (119, 140), and to decode electrophysiologic population dynamics from microensemble activity (106, 107).

Collectively, functional optical imaging modalities have immense scalability, to image at the micro-, meso- and macro-circuit level,

allowing inference to be drawn about the interplay between the cellular and network evolution of seizures (17, 18, 66). While we think about a classic seizure as evolving, massive hypersynchronous activity, largely due to the use of EEG to identify and study these dynamics, functional optical imaging has made it abundantly clear that while that certainly is a defining feature, there are intricate activity patterns across cell types precipitating and underlying these events.

Author contributions

MS: Conceptualization, Data curation, Formal analysis, Funding acquisition, Investigation, Methodology, Project administration, Resources, Software, Visualization, Writing – original draft, Writing – review & editing. RD: Validation, Writing – review & editing. RG: Conceptualization, Funding acquisition, Resources, Supervision, Validation, Writing – review & editing. KB: Conceptualization, Data curation, Funding acquisition, Resources, Supervision, Validation, Visualization, Writing – review & editing.

Funding

The author(s) declare financial support was received for the research, authorship, and/or publication of this article. This work was

References

- Chadwick D, Taylor J, Johnson T. Outcomes after seizure recurrence in people with well-controlled epilepsy and the factors that influence it. *Epilepsia*. (1996) 37:1043–50. doi: 10.1111/j.1528-1157.1996.tb01023.x
- Hauser WA, Rich SS, Lee JR, Annegers JF, Anderson VE. Risk of recurrent seizures after two unprovoked seizures. *N Engl J Med*. (1998) 338:429–34. doi: 10.1056/NEJM199802123380704
- Fisher RS, Acevedo C, Arzimanoglou A, Bogacz A, Cross JH, Elger CE, et al. ILAE official report: a practical clinical definition of epilepsy. *Epilepsia*. (2014) 55:475–82. doi: 10.1111/epi.12550
- Hirtz D, Thurman DJ, Gwinn-Hardy K, Mohamed M, Chaudhuri AR, Zalutsky R. How common are the “common” neurologic disorders? *Neurology*. (2007) 68:326–37. doi: 10.1212/01.wnl.0000252807.38124.a3
- Zack MM, Kobau R. National and state estimates of the numbers of adults and children with active epilepsy - United States, 2015. *Morbidity Mortality Weekly Rep*. (2017) 66:821–5. doi: 10.15585/mmwr.mm6631a1
- Beghi E, Giussani G, Abd-Allah F, Abdela J, Abdelalim A, Abraha HN, et al. Global, regional, and national burden of epilepsy, 1990–2016: a systematic analysis for the global burden of disease study 2016. *Lancet Neurol*. (2019) 18:357–75. doi: 10.1016/S1474-4422(18)30454-X
- Rho JM, White HS. Brief history of anti-seizure drug development. *Epilepsia Open*. (2018) 3:114–9. doi: 10.1002/epi4.12268
- Hauser WA, Kurland LT. Epidemiology of epilepsy in Rochester, Minnesota, 1935 through 1967. *Epilepsia*. (1975) 16:1–66. doi: 10.1111/j.1528-1157.1975.tb04721.x
- Kwan P, Brodie MJ. Early identification of refractory epilepsy. *N Engl J Med*. (2000) 342:314–9. doi: 10.1056/NEJM200002033420503
- Kwan P, Sperling MR. Refractory seizures: try additional antiepileptic drugs (after two have failed) or go directly to early surgery evaluation? *Epilepsia*. (2009) 50:57–62. doi: 10.1111/j.1528-1167.2009.02237.x
- Gross RE, Stern MA, Willie JT, Fasano RE, Saindane AM, Soares BP, et al. Stereotactic laser amygdalohippocampotomy for mesial temporal lobe epilepsy. *Ann Neurol*. (2018) 83:575–87. doi: 10.1002/ana.25180
- Wu CY, Jermakowicz WJ, Chakravorti S, Cajigas I, Sharan AD, Jagid JR, et al. Effects of surgical targeting in laser interstitial thermal therapy for mesial temporal lobe epilepsy: a multicenter study of 234 patients. *Epilepsia*. (2019) 60:1171–83. doi: 10.1111/epi.15565
- Wiebe S, Blume WT, Girvin JP, Eliasziw M. Effectiveness and Efficiency of Surgery for Temporal Lobe Epilepsy Study Group. A randomized, controlled trial of surgery for

supported by the National Institute of Health grants F31NS115479 to MAS and R21NS112948 and R21NS132071 to REG, in addition to funding provided by the Mirowski Family Foundation to REG.

Acknowledgments

We thank Bona Kim for her illustration work.

Conflict of interest

The authors declare that the research was conducted in the absence of any commercial or financial relationships that could be construed as a potential conflict of interest.

Publisher's note

All claims expressed in this article are solely those of the authors and do not necessarily represent those of their affiliated organizations, or those of the publisher, the editors and the reviewers. Any product that may be evaluated in this article, or claim that may be made by its manufacturer, is not guaranteed or endorsed by the publisher.

temporal-lobe epilepsy. *N Engl J Med*. (2001) 345:311–8. doi: 10.1056/NEJM200108023450501

14. Josephson CB, Dykeman J, Fiest KM, Liu X, Sadler RM, Jette N, et al. Systematic review and meta-analysis of standard vs selective temporal lobe epilepsy surgery. *Neurology*. (2013) 80:1669–76. doi: 10.1212/WNL.0b013e3182904f82

15. Salanova V, Witt T, Worth R, Henry TR, Gross RE, Nazzaro JM, et al. Long-term efficacy and safety of thalamic stimulation for drug-resistant partial epilepsy. *Neurology*. (2015) 84:1017–25. doi: 10.1212/WNL.0000000000001334

16. Heck CN, King-Stephens D, Massey AD, Nair DR, Jobst BC, Barkley GL, et al. Two-year seizure reduction in adults with medically intractable partial onset epilepsy treated with responsive neurostimulation: final results of the RNS system pivotal trial. *Epilepsia*. (2014) 55:432–41. doi: 10.1111/epi.12534

17. Rossi LF, Kullmann DM, Wykes RC. The enlightened brain: novel imaging methods focus on epileptic networks at multiple scales. *Front Cell Neurosci*. (2018) 12:1–8. doi: 10.3389/fncel.2018.00082

18. Farrell JS, Nguyen QA, Soltesz I. Resolving the Micro-macro disconnect to address Core features of seizure networks. *Neuron*. (2019) 101:1016–28. doi: 10.1016/j.neuron.2019.01.043

19. Schevon CA, Weiss SA, McKhann G, Goodman RR, Yuste R, Emerson RG, et al. Evidence of an inhibitory restraint of seizure activity in humans. *Nat Commun*. (2012) 3:1060. doi: 10.1038/ncomms2056

20. Truccolo W, Donoghue JA, Hochberg LR, Eskandar EN, Madsen JR, Anderson WS, et al. Single-neuron dynamics in human focal epilepsy. *Nat Neurosci*. (2011) 14:635–41. doi: 10.1038/nn.2782

21. Truccolo W, Ahmed OJ, Harrison MT, Eskandar EN, Cosgrove GR, Madsen JR, et al. Neuronal ensemble synchrony during human focal seizures. *J Neurosci*. (2014) 34:9927–44. doi: 10.1523/JNEUROSCI.4567-13.2014

22. Smith EH, Liou YY, Merricks EM, Davis T, Thomson K, Greger B, et al. Human interictal epileptiform discharges are bidirectional traveling waves echoing ictal discharges. *Elife*. (2022) 11:20. doi: 10.7554/eLife.73541

23. Liou JY, Ma HT, Wenzel M, Zhao MR, Baird-Daniel E, Smith EH, et al. Role of inhibitory control in modulating focal seizure spread. *Brain*. (2018) 141:2083–97. doi: 10.1093/brain/awy116

24. Trevelyan AJ, Schevon CA. How inhibition influences seizure propagation. *Neuropharmacology*. (2013) 69:45–54. doi: 10.1016/j.neuropharm.2012.06.015

25. Neumann AR, Raedt R, Steenland HW, Sprengers M, Bzymek K, Navratilova Z, et al. Involvement of fast-spiking cells in ictal sequences during spontaneous seizures in

- rats with chronic temporal lobe epilepsy. *Brain*. (2017) 140:2355–69. doi: 10.1093/brain/awx179
26. Miri ML, Vinck M, Pant R, Cardin JA. Altered hippocampal interneuron activity precedes ictal onset. *eLife*. (2018) 7:20. doi: 10.7554/eLife.40750
27. Trevelyan AJ, Sussillo D, Watson BO, Yuste R. Modular propagation of epileptiform activity: evidence for an inhibitory veto in neocortex. *J Neurosci*. (2006) 26:12447–55. doi: 10.1523/JNEUROSCI.2787-06.2006
28. Trevelyan AJ, Sussillo D, Yuste R. Feedforward inhibition contributes to the control of epileptiform propagation speed. *J Neurosci*. (2007) 27:3383–7. doi: 10.1523/JNEUROSCI.0145-07.2007
29. Baird-Daniel E, Daniel AGS, Wenzel M, Li D, Liou JY, Laffont P, et al. Glial calcium waves are triggered by seizure activity and not essential for initiating ictal onset or neurovascular coupling. *Cereb Cortex*. (2017) 27:3318–30. doi: 10.1093/cercor/bhx072
30. Muldoon SF, Soltesz I, Cossart R. Spatially clustered neuronal assemblies comprise the microstructure of synchrony in chronically epileptic networks. *Proc Natl Acad Sci U S A*. (2013) 110:3567–72. doi: 10.1073/pnas.1216958110
31. Ma HT, Wu CH, Wu JY. Initiation of spontaneous epileptiform events in the rat neocortex in vivo. *J Neurophysiol*. (2004) 91:934–45. doi: 10.1152/jn.00274.2003
32. Ma HT, Zhao MR, Schwartz TH. Dynamic neurovascular coupling and uncoupling during ictal onset, propagation, and termination revealed by simultaneous in vivo optical imaging of neural activity and local blood volume. *Cereb Cortex*. (2013) 23:885–99. doi: 10.1093/cercor/bhs079
33. Tsytsarev V, Sopova JV, Leonova EI, Inyushin M, Markina AA, Chirinskaite AV, et al. Neurophotonic methods in approach to in vivo animal epileptic models: advantages and limitations. *Epilepsia*. (2024) 65:600–14. doi: 10.1111/epi.17870
34. Rodriguez EA, Campbell RE, Lin JY, Lin MZ, Miyawaki A, Palmer AE, et al. The growing and glowing toolbox of fluorescent and photoactive proteins. *Trends Biochem Sci*. (2017) 42:111–29. doi: 10.1016/j.tibs.2016.09.010
35. Akerboom J, Rivera JDV, Guilbe MMR, Malave ECA, Hernandez HH, Tian L, et al. Crystal structures of the GCaMP calcium sensor reveal the mechanism of fluorescence signal change and aid rational design. *J Biol Chem*. (2009) 284:6455–64. doi: 10.1074/jbc.M807657200
36. Nagai T, Sawano A, Park ES, Miyawaki A. Circularly permuted green fluorescent proteins engineered to sense Ca²⁺. *Proc Natl Acad Sci USA*. (2001) 98:3197–202. doi: 10.1073/pnas.051636098
37. Dana H, Sun Y, Mohar B, Hulse BK, Kerlin AM, Hasseman JP, et al. High-performance calcium sensors for imaging activity in neuronal populations and microcompartments. *Nat Methods*. (2019) 16:649–57. doi: 10.1038/s41592-019-0435-6
38. Dana H, Mohar B, Sun Y, Narayan S, Gordus A, Hasseman JP, et al. Sensitive red protein calcium indicators for imaging neural activity. *eLife*. (2016) 5:24. doi: 10.7554/eLife.12727
39. Mohr MA, Bushey D, Aggarwal A, Marvin JS, Kim JJ, Marquez EJ, et al. jRCaMP1: an optimized calcium indicator for two-photon imaging at fiber laser wavelengths. *Nat Methods*. (2020) 17:694–7. doi: 10.1038/s41592-020-0835-7
40. Inoue M, Takeuchi A, Manita S, Horigane S, Sakamoto M, Kawakami R, et al. Rational engineering of XCaMPs, a multicolor GECI suite for in vivo imaging of complex brain circuit dynamics. *Cell*. (2019) 177:1346–1360.e24. doi: 10.1016/j.cell.2019.04.007
41. Qian Y, Piatkevich KD, Mc Larney B, Abdelfattah AS, Mehta S, Murdock MH, et al. A genetically encoded near-infrared fluorescent calcium ion indicator. *Nat Methods*. (2019) 16:171–4. doi: 10.1038/s41592-018-0294-6
42. Sabatini BL, Tian L. Imaging neurotransmitter and neuromodulator dynamics in vivo with genetically encoded indicators. *Neuron*. (2020) 108:17–32. doi: 10.1016/j.neuron.2020.09.036
43. Berglund K, Wen L, Dunbar RL, Feng GP, Augustine GJ. Optogenetic visualization of presynaptic tonic inhibition of cerebellar parallel fibers. *J Neurosci*. (2016) 36:5709–23. doi: 10.1523/JNEUROSCI.4366-15.2016
44. Sato SS, Artoni P, Landi S, Cozzolino O, Parra R, Pracucci E, et al. Simultaneous two-photon imaging of intracellular chloride concentration and pH in mouse pyramidal neurons in vivo. *Proc Natl Acad Sci USA*. (2017) 114:E8770–9. doi: 10.1073/pnas.1702861114
45. Bischof H, Rehberg M, Stryeck S, Artinger K, Eroglu E, Waldeck-Weiermair M, et al. Novel genetically encoded fluorescent probes enable real-time detection of potassium in vitro and in vivo. *Nat Commun*. (2017) 8:12. doi: 10.1038/s41467-017-01615-z
46. Shen Y, Wu SY, Rancic V, Aggarwal A, Qian Y, Miyashita SI, et al. Genetically encoded fluorescent indicators for imaging intracellular potassium ion concentration. *Commun Biol*. (2019) 2:10. doi: 10.1038/s42003-018-0269-2
47. Cabán CCT, Yang MH, Lai CX, Yang LN, Subach FV, Smith BO, et al. Tuning the sensitivity of genetically encoded fluorescent potassium indicators through structure-guided and genome mining strategies. *ACS Sensors*. (2022) 7:1336–46. doi: 10.1021/acssensors.1c02201
48. Rossano AJ, Chouhan AK, Macleod GT. Genetically encoded pH-indicators reveal activity-dependent cytosolic acidification of Drosophila motor nerve termini in vivo. *J Physiol*. (2013) 591:1691–706. doi: 10.1113/jphysiol.2012.248377
49. Marvin JS, Borghuis BG, Tian L, Cichon J, Harnett MT, Akerboom J, et al. An optimized fluorescent probe for visualizing glutamate neurotransmission. *Nat Methods*. (2013) 10:162–70. doi: 10.1038/nmeth.2333
50. Marvin JS, Scholl B, Wilson DE, Podgurski K, Kazempour A, Müller JA, et al. Stability, affinity, and chromatic variants of the glutamate sensor iGluSnFR. *Nat Methods*. (2018) 15:936–9. doi: 10.1038/s41592-018-0171-3
51. Marvin JS, Shimoda Y, Magloire V, Leite M, Kawashima T, Jensen TP, et al. A genetically encoded fluorescent sensor for in vivo imaging of GABA. *Nat Methods*. (2019) 16:763–70. doi: 10.1038/s41592-019-0471-2
52. Sun FM, Zeng JZ, Jing M, Zhou JH, Feng JS, Owen SF, et al. A genetically encoded fluorescent sensor enables rapid and specific detection of dopamine in flies, fish, and mice. *Cell*. (2018) 174:481–496.e19. doi: 10.1016/j.cell.2018.06.042
53. Patriarchi T, Cho JR, Merten K, Howe MW, Marley A, Xiong WH, et al. Ultrafast neuronal imaging of dopamine dynamics with designed genetically encoded sensors. *Science*. (2018) 360:eaat4422. doi: 10.1126/science.aat4422
54. Deng F, Wan JX, Li GC, Dong H, Xia XJ, Wang YP, et al. Improved green and red GRAB sensors for monitoring spatiotemporal serotonin release in vivo. *Nat Methods*. (2024) 21:692–702. doi: 10.1038/s41592-024-02188-8
55. Unger EK, Keller JP, Altermatt M, Liang RQ, Matsui A, Dong CY, et al. Directed evolution of a selective and sensitive serotonin sensor via machine learning. *Cell*. (2020) 183:1986–2002.e26. doi: 10.1016/j.cell.2020.11.040
56. Dong A, He KK, Dudok B, Farrell JS, Guan WQ, Liput DJ, et al. A fluorescent sensor for spatiotemporally resolved imaging of endocannabinoid dynamics in vivo. *Nat Biotechnol*. (2022) 40:787–98. doi: 10.1038/s41587-021-01074-4
57. Borden PM, Zhang P, Shivange AV, Marvin JS, Cichon J, Dan C, et al. A fast genetically encoded fluorescent sensor for faithful in vivo acetylcholine detection in mice, fish, worms and flies. *bioRxiv*. (2020) 2020.02.07.939504
58. Lobas MA, Tao R, Nagai J, Kronschräger MT, Borden PM, Marvin JS, et al. A genetically encoded single-wavelength sensor for imaging cytosolic and cell surface ATP. *Nat Commun*. (2019) 10:13. doi: 10.1038/s41467-019-08441-5
59. Bando Y, Sakamoto M, Kim S, Ayzenshtat I, Yuste R. Comparative evaluation of genetically encoded voltage indicators. *Cell Rep*. (2019) 26:802–813.e4. doi: 10.1016/j.celrep.2018.12.088
60. Liu ZH, Lu XY, Villette V, Gou YY, Colbert KL, Lai SJ, et al. Sustained deep-tissue voltage recording using a fast indicator evolved for two-photon microscopy. *Cell*. (2022) 185:3408–3425.e29. doi: 10.1016/j.cell.2022.07.013
61. Gong YY, Huang C, Li JZ, Grewe BF, Zhang YP, Eismann S, et al. High-speed recording of neural spikes in awake mice and flies with a fluorescent voltage sensor. *Science*. (2015) 350:1361–6. doi: 10.1126/science.aab0810
62. Adam Y, Kim JJ, Lou S, Zhao YX, Xie ME, Brinks D, et al. Voltage imaging and optogenetics reveal behaviour-dependent changes in hippocampal dynamics. *Nature*. (2019) 569:413–7. doi: 10.1038/s41586-019-1166-7
63. Abdelfattah AS, Kawashima T, Singh A, Novak O, Liu H, Shuai YC, et al. Bright and photostable chemogenetic indicators for extended in vivo voltage imaging. *Science*. (2019) 365:699–704. doi: 10.1126/science.aav6416
64. Benninger RKP, Piston DW. Two-photon excitation microscopy for the study of living cells and tissues. *Curr Protoc Cell Biol*. (2013) Chapter 4:4.11.1–4.11.24. doi: 10.1002/0471143030.cb0411s59
65. Hillman EMC, Voleti V, Li WZ, Yu H. Light-sheet microscopy in neuroscience. In: B Roska and HY Zoghbi, editors. Annual review of neuroscience, vol. 42. Palo Alto: Annual Reviews (2019). 295–313.
66. Lawlor PN, Goldberg EM. Dynamic fluorescence imaging in experimental epilepsy. *Epilepsy Curr*. (2022) 22:364–71. doi: 10.1177/1535759722113436
67. Helmchen F, Denk W. Deep tissue two-photon microscopy. *Nat Methods*. (2005) 2:932–40. doi: 10.1038/nmeth818
68. Svoboda K, Yasuda R. Principles of two-photon excitation microscopy and its applications to neuroscience. *Neuron*. (2006) 50:823–39. doi: 10.1016/j.neuron.2006.05.019
69. Ghosh KK, Burns LD, Cocker ED, Nimmerjahn A, Ziv Y, El Gamal A, et al. Miniaturized integration of a fluorescence microscope. *Nat Methods*. (2011) 8:871–8. doi: 10.1038/nmeth.1694
70. Helmchen F, Fee MS, Tank DW, Denk W. A miniature head-mounted two-photon microscope: high-resolution brain imaging in freely moving animals. *Neuron*. (2001) 31:903–12. doi: 10.1016/S0896-6273(01)00421-4
71. Zong WJ, Wu RL, Li ML, Hu YH, Li YJ, Li JH, et al. Fast high-resolution miniature two-photon microscopy for brain imaging in freely behaving mice. *Nat Methods*. (2017) 14:713–9. doi: 10.1038/nmeth.4305
72. Muldoon SF, Villette V, Tressard T, Malvache A, Reichinnek S, Bartolomei F, et al. GABAergic inhibition shapes interictal dynamics in awake epileptic mice. *Brain*. (2015) 138:2875–90. doi: 10.1093/brain/awv227
73. de Curtis M, Avanzini G. Interictal spikes in focal epileptogenesis. *Prog Neurobiol*. (2001) 63:541–67. doi: 10.1016/S0304-0082(00)00026-5
74. Rossi LF, Wykes RC, Kullmann DM, Carandini M. Focal cortical seizures start as standing waves and propagate respecting homotopic connectivity. *Nat Commun*. (2017) 8:1–11. doi: 10.1038/s41467-017-00159-6

75. Steinmetz NA, Buetfering C, Lecoq J, Lee CR, Peters AJ, Jacobs EAK, et al. Aberrant cortical activity in multiple GCaMP6-expressing transgenic mouse lines. *eNeuro*. (2017) 4:ENEURO.0207-17.2017. doi: 10.1523/ENEURO.0207-17.2017
76. Montgomery MK, Kim SH, Dovas A, Zhao HZT, Goldberg AR, Xu WH, et al. Glioma-induced alterations in neuronal activity and neurovascular coupling during disease progression. *Cell Rep*. (2020) 31:107500. doi: 10.1016/j.celrep.2020.03.064
77. Luo PJ, Yang F, Li J, Niemeier JE, Zhan FR, Estin J, et al. Excitatory-inhibitory mismatch shapes node recruitment in an epileptic network. *Epilepsia*. (2023) 64:1939–50. doi: 10.1111/epi.17638
78. Cozzolino O, Sicca F, Paoli E, Trovato F, Santorelli FM, Ratto GM, et al. Evolution of epileptiform activity in zebrafish by statistical-based integration of electrophysiology and 2-photon calcium imaging. *Cells*. (2020) 9:19. doi: 10.3390/cells9030769
79. Liu J, Salvati KA, Baraban SC. In vivo calcium imaging reveals disordered interictal network dynamics in epileptic *stxbp1b* zebrafish. *iScience*. (2021) 24:102558. doi: 10.1016/j.isci.2021.102558
80. Niemeier JE, Gadumsetty P, Chun C, Sylvester S, Lucas JP, Ma HC, et al. Seizures initiate in zones of relative hyperexcitation in a zebrafish epilepsy model. *Brain*. (2022) 145:2347–60. doi: 10.1093/brain/awac073
81. Liu J, Baraban SC. Network properties revealed during multi-scale calcium imaging of seizure activity in zebrafish. *eNeuro*. (2019) 6:ENEURO.0041-19.2019. doi: 10.1523/ENEURO.0041-19.2019
82. Masala N, Pofahl M, Haubrich AN, Islam KUS, Nikbakht N, Pasdarnavab M, et al. Targeting aberrant dendritic integration to treat cognitive comorbidities of epilepsy. *Brain*. (2023) 146:2399–417. doi: 10.1093/brain/awac455
83. Sparks FT, Liao Z, Li W, Grosmark A, Soltesz I, Losonczy A. Hippocampal adult-born granule cells drive network activity in a mouse model of chronic temporal lobe epilepsy. *Nat Commun*. (2020) 11:13. doi: 10.1038/s41467-020-19969-2
84. Hadjiabadi D, Lovett-Barron M, Raikov IG, Sparks FT, Liao ZR, Baraban SC, et al. Maximally selective single-cell target for circuit control in epilepsy models. *Neuron*. (2021) 109:2556–2572.e6. doi: 10.1016/j.neuron.2021.06.007
85. Jamiolkowski RM, Nguyen QA, Farrell JS, McGinn RJ, Hartmann DA, Nirschl JJ, et al. The fasciola cinereum of the hippocampal tail as an interventional target in epilepsy. *Nat Med*. (2024) 30:1292–9. doi: 10.1038/s41591-024-02924-9
86. Heuser K, Nome CG, Pettersen KH, Åbjorsbråten KS, Jensen V, Tang WN, et al. Ca²⁺ signals in astrocytes facilitate spread of epileptiform activity. *Cereb Cortex*. (2018) 28:4036–48. doi: 10.1093/cercor/bhy196
87. Petrucco L, Pracucci E, Brondi M, Ratto GM, Landi S. Epileptiform activity in the mouse visual cortex interferes with cortical processing in connected areas. *Sci Rep*. (2017) 7:40054. doi: 10.1038/srep40054
88. Li M, Eltabbal M, Tran HD, Kuhn B. Scn2a insufficiency alters spontaneous neuronal Ca²⁺ activity in somatosensory cortex wakefulness. *iScience*. (2023) 26:108138. doi: 10.1016/j.isci.2023.108138
89. Aeed F, Shnitzer T, Talmon R, Schiller Y. Layer- and cell-specific recruitment dynamics during epileptic seizures in vivo. *Ann Neurol*. (2020) 87:97–115. doi: 10.1002/ana.25628
90. Bando Y, Wenzel M, Yuste R. Simultaneous two-photon imaging of action potentials and subthreshold inputs in vivo. *Nat Commun*. (2021) 12:12. doi: 10.1038/s41467-021-27444-9
91. Shimoda Y, Leite M, Graham RT, Marvin JS, Hasseman J, Kolb I, et al. Extracellular glutamate and GABA transients at the transition from interictal spiking to seizures. *Brain*. (2024) 147:1011–24. doi: 10.1093/brain/awad336
92. Magloire V, Mercier MS, Kullmann DM, Pavlov I. GABAergic interneurons in seizures: investigating causality with Optogenetics. *Neuroscientist*. (2019) 25:344–58. doi: 10.1177/1073858418805002
93. Li J, Yang F, Zhan FR, Estin J, Iyer A, Zhao MR, et al. Mesoscopic mapping of hemodynamic responses and neuronal activity during pharmacologically induced interictal spikes in awake and anesthetized mice. *J Cereb Blood Flow Metab*. (2024) 44:911–24. doi: 10.1177/0271678X241226742
94. Shuman T, Aharoni D, Cai DJ, Lee CR, Chavlis S, Page-Harley L, et al. Breakdown of spatial coding and interneuron synchronization in epileptic mice. *Nat Neurosci*. (2020) 23:229–38. doi: 10.1038/s41593-019-0559-0
95. Wenzel M, Hamm JP, Peterka DS, Yuste R. Acute focal seizures start as local synchronizations of neuronal ensembles. *J Neurosci*. (2019) 39:8562–75. doi: 10.1523/JNEUROSCI.3176-18.2019
96. Brevet A, Hassan-Abdi R, Somkhit J, Yanicostas C, Soussi-Yanicostas N. Defective excitatory/inhibitory synaptic balance and increased neuron apoptosis in a zebrafish model of Dravet syndrome. *Cells*. (2019) 8:13. doi: 10.3390/cells8101199
97. Liao MJ, Kundap U, Rosch RE, Burrows DRW, Meyer MP, Bencheikh BOA, et al. Targeted knockout of GABA-A receptor gamma 2 subunit provokes transient light-induced reflex seizures in zebrafish larvae. *Dis Model Mech*. (2019) 12:11. doi: 10.1242/dmm.040782
98. Verdugo CD, Myren-Svelstad S, Aydin E, Van Hoeymissen E, Deneubourg C, Vanderhaeghe S, et al. Glia-neuron interactions underlie state transitions to generalized seizures. *Nat Commun*. (2019) 10:13. doi: 10.1038/s41467-019-11739-z
99. Turrini L, Sorelli M, de Vito G, Credi C, Tiso N, Vanzi F, et al. Multimodal characterization of seizures in zebrafish larvae. *Biomedicines*. (2022) 10:16. doi: 10.3390/biomedicines10050951
100. Hotz AL, Jamali A, Rieser NN, Niklaus S, Aydin E, Myren-Svelstad S, et al. Loss of glutamate transporter *eaat2a* leads to aberrant neuronal excitability, recurrent epileptic seizures, and basal hypoactivity. *Glia*. (2022) 70:196–214. doi: 10.1002/glia.24106
101. Myren-Svelstad S, Jamali A, Ophus SS, D'Gama PP, Ostenrath AM, Mutlu AK, et al. Elevated photic response is followed by a rapid decay and depressed state in ictogenic networks. *Epilepsia*. (2022) 63:2543–60. doi: 10.1111/epi.17380
102. Tran CH, Vaiana M, Nakuci J, Somarowthu A, Goff KM, Goldstein N, et al. Interneuron desynchronization precedes seizures in a mouse model of Dravet syndrome. *J Neurosci*. (2020) 40:2764–75. doi: 10.1523/JNEUROSCI.2370-19.2020
103. Lim HK, You N, Bae S, Kang BM, Shon YM, Kim SG, et al. Differential contribution of excitatory and inhibitory neurons in shaping neurovascular coupling in different epileptic neural states. *J Cereb Blood Flow Metab*. (2021) 41:1145–61. doi: 10.1177/0271678X20934071
104. Rosch RE, Hunter PR, Baldeweg T, Friston KJ, Meyer MP. Calcium imaging and dynamic causal modelling reveal brain-wide changes in effective connectivity and synaptic dynamics during epileptic seizures. *PLoS Comput Biol*. (2018) 14:23. doi: 10.1371/journal.pcbi.1006375
105. Burrows DRW, Diana G, Pimpel B, Moeller F, Richardson MP, Bassett DS, et al. Microscale neuronal activity collectively drives chaotic and inflexible dynamics at the macroscale in seizures. *J Neurosci*. (2023) 43:3259–83. doi: 10.1523/JNEUROSCI.0171-22.2023
106. Zhang J, Liu XJ, Xu WJ, Luo WH, Li M, Chu FB, et al. Stretchable transparent electrode arrays for simultaneous electrical and optical interrogation of neural circuits in vivo. *Nano Lett*. (2018) 18:2903–11. doi: 10.1021/acs.nanolett.8b00087
107. Driscoll N, Rosch RE, Murphy BB, Ashourvan A, Vishnubhotla R, Dickens OO, et al. Multimodal in vivo recording using transparent graphene microelectrodes illuminates spatiotemporal seizure dynamics at the microscale. *Commun Biol*. (2021) 4:14. doi: 10.1038/s42003-021-01670-9
108. Mulcahey PJ, Chen YZ, Driscoll N, Murphy BB, Dickens OO, Johnson ATC, et al. Multimodal, multiscale insights into hippocampal seizures enabled by transparent, graphene-based microelectrode arrays. *eNeuro*. (2022) 9:ENEURO.0386-21.2022. doi: 10.1523/ENEURO.0386-21.2022
109. Zhang ZR, Jiang SH, Shi KB, Li Y, Jin WN, Liu Q, et al. Visualizing seizure propagation in freely-moving mice via miniature two-photon microscopy. *Neurosci Bull*. (2022) 38:1593–7. doi: 10.1007/s12264-022-00947-1
110. Wong JC, Grieco SF, Dutt K, Chen LJ, Thelin JT, Inglis GAS, et al. Autistic-like behavior, spontaneous seizures, and increased neuronal excitability in a *Scn8a* mouse model. *Neuropsychopharmacology*. (2021) 46:2011–20. doi: 10.1038/s41386-021-00985-9
111. Stern MA, Cole ER, Gross RE, Berglund K. Seizure event detection using intravital two-photon calcium imaging data. *Neurophotonics*. (2024) 11:024202. doi: 10.1117/1.NPh.11.2.024202
112. Jayant K, Wenzel M, Bando Y, Hamm JP, Mandriota N, Rabinowitz JH, et al. Flexible Nanopipettes for minimally invasive intracellular electrophysiology in vivo. *Cell Rep*. (2019) 26:266–278.e5. doi: 10.1016/j.celrep.2018.12.019
113. Wenzel M, Hamm JP, Peterka DS, Yuste R. Reliable and elastic propagation of cortical seizures in vivo. *Cell Rep*. (2017) 19:2681–93. doi: 10.1016/j.celrep.2017.05.090
114. Shah PT, Valiante TA, Packer AM. Highly local activation of inhibition at the seizure wavefront in vivo. *Cell Rep*. (2024) 43:114189. doi: 10.1016/j.celrep.2024.114189
115. Somarowthu A, Goff KM, Goldberg EM. Two-photon calcium imaging of seizures in awake, head-fixed mice. *Cell Calcium*. (2021) 96:102380. doi: 10.1016/j.ceca.2021.102380
116. Yang F, Li J, Song Y, Zhao MR, Niemeier JE, Luo PJ, et al. Mesoscopic mapping of ictal neurovascular coupling in awake behaving mice using optical spectroscopy and genetically encoded calcium indicators. *Front Neurosci*. (2021) 15:704834. doi: 10.3389/fnins.2021.704834
117. Hatcher A, Yu K, Meyer J, Aiba I, Deneen B, Noebels JL. Pathogenesis of peritumoral hyperexcitability in an immunocompetent CRISPR-based glioblastoma model. *J Clin Invest*. (2020) 130:2286–300. doi: 10.1172/JCI133316
118. de Vito G, Turrini L, Müllenbroich C, Ricci P, Sancataldo G, Mazzamuto G, et al. Fast whole-brain imaging of seizures in zebrafish larvae by two-photon light-sheet microscopy. *Biomed Opt Express*. (2022) 13:1516–36. doi: 10.1364/BOE.434146
119. Özsoy Ç, Hotz AL, Rieser NN, Chen ZY, Deán-Ben XL, Neuhaus SCF, et al. Volumetric optoacoustic neurobehavioral tracking of epileptic seizures in freely-swimming zebrafish larvae. *Front Mol Neurosci*. (2022) 15:9. doi: 10.3389/fnmol.2022.1004518
120. Turrini L, Fornetto C, Marchetto G, Müllenbroich MC, Tiso N, Vettori A, et al. Optical mapping of neuronal activity during seizures in zebrafish. *Sci Rep*. (2017) 7:12. doi: 10.1038/s41598-017-03087-z
121. Winter MJ, Windell D, Metz J, Matthews P, Pinion J, Brown JT, et al. 4-dimensional functional profiling in the convulsant-treated larval zebrafish brain. *Sci Rep*. (2017) 7:16. doi: 10.1038/s41598-017-06646-6

122. Meyer J, Maheshwari A, Noebels J, Smirnakis S. Asynchronous suppression of visual cortex during absence seizures in stargazer mice. *Nat Commun.* (2018) 9:9. doi: 10.1038/s41467-018-04349-8
123. Berdyeva TK, Frady EP, Nassi JJ, Aluisio L, Cherkas Y, Otte S, et al. Direct imaging of hippocampal epileptiform calcium motifs following Kainic acid Administration in Freely Behaving Mice. *Front Neurosci.* (2016) 10:53. doi: 10.3389/fnins.2016.00053
124. Farrell JS, Colangeli R, Dudok B, Wolff MD, Nguyen SL, Jackson J, et al. In vivo assessment of mechanisms underlying the neurovascular basis of postictal amnesia. *Sci Rep.* (2020) 10:13. doi: 10.1038/s41598-020-71935-6
125. Lau LA, Zhao Z, Gomperts SN, Staley KJ, Lillis KP. Cellular resolution contributions to ictal population signals. *Epilepsia.* (2024) 65:2165–78. doi: 10.1111/epi.17983
126. Farrell JS, Colangeli R, Dong A, George AG, Addo-Osafo K, Kingsley PJ, et al. In vivo endocannabinoid dynamics at the timescale of physiological and pathological neural activity. *Neuron.* (2021) 109:2398–2403.e4. doi: 10.1016/j.neuron.2021.05.026
127. Nguyen QA, Klein PM, Xie C, Benthall KN, Iafrafi J, Homidan J, et al. Acetylcholine receptor based chemogenetics engineered for neuronal inhibition and seizure control assessed in mice. *Nat Commun.* (2024) 15:13. doi: 10.1038/s41467-024-44853-8
128. Enger R, Tang WN, Vindedal GF, Jensen V, Helm PJ, Sprengel R, et al. Dynamics of ionic shifts in cortical spreading depression. *Cereb Cortex.* (2015) 25:4469–76. doi: 10.1093/cercor/bhv054
129. Tamim I, Chung DY, de Morais AL, Loonen ICM, Qin T, Misra A, et al. Spreading depression as an innate antiseizure mechanism. *Nat Commun.* (2021) 12:1–15. doi: 10.1038/s41467-021-22464-x
130. Dreier JP, Major S, Pannek HW, Woitzik J, Scheel M, Wiesenthal D, et al. Spreading convulsions, spreading depolarization and epileptogenesis in human cerebral cortex. *Brain.* (2012) 135:259–75. doi: 10.1093/brain/awr303
131. Tran CH, George AG, Teskey GC, Gordon GR. Seizures elevate gliovascular unit Ca²⁺ and cause sustained vasoconstriction. *JCI Insight.* (2020) 5:12. doi: 10.1172/jci.insight.136469
132. Schevon CA, Goodman RR, McKhann G, Emerson RG. Propagation of epileptiform activity on a submillimeter scale. *J Clin Neurophysiol.* (2010) 27:406–11. doi: 10.1097/WNP.0b013e3181fd8a1
133. Stead M, Bower M, Brinkmann BH, Lee K, Marsh WR, Meyer FB, et al. Microseizures and the spatiotemporal scales of human partial epilepsy. *Brain.* (2010) 133:2789–97. doi: 10.1093/brain/awq190
134. Prince DA, Wilder BJ. Control mechanisms in cortical epileptogenic foci - "surround" inhibition. *Arch Neurol.* (1967) 16:194–202. doi: 10.1001/archneur.1967.00470200082007
135. Khan L, van Lanen R, Hoogland G, Schijns O, Rijkers K, Kapsokalyvas D, et al. Two-photon imaging to unravel the Pathomechanisms associated with epileptic seizures: a review. *Appl Sci.* (2021) 11:24. doi: 10.3390/app11052404
136. Lieb A, Qiu YC, Dixon CL, Heller JP, Walker MC, Schorge S, et al. Biochemical autoregulatory gene therapy for focal epilepsy. *Nat Med.* (2018) 24:1324–9. doi: 10.1038/s41591-018-0103-x
137. Kim TH, Zhang YP, Lecoq J, Jung JC, Li J, Zeng HK, et al. Long-term optical access to an estimated one million neurons in the live mouse cortex. *Cell Rep.* (2016) 17:3385–94. doi: 10.1016/j.celrep.2016.12.004
138. Ichimura T, Kakizuka T, Horikawa K, Seiriki K, Kasai A, Hashimoto H, et al. Exploring rare cellular activity in more than one million cells by a transscale scope. *Sci Rep.* (2021) 11:16. doi: 10.1038/s41598-021-95930-7
139. Horton NG, Wang K, Kobat D, Clark CG, Wise FW, Schaffer CB, et al. In vivo three-photon microscopy of subcortical structures within an intact mouse brain. *Nat Photonics.* (2013) 7:205–9. doi: 10.1038/nphoton.2012.336
140. Zong WJ, Obenaus HA, Skytoen ER, Eneqvist H, de Jong NL, Vale R, et al. Large-scale two-photon calcium imaging in freely moving mice. *Cell.* (2022) 185:1240–1256.e30. doi: 10.1016/j.cell.2022.02.017